

AN ALGORITHM FOR ACCURATE MEASUREMENT OF CORNEAL THICKNESS USING ULTRASOUND rf SIGNAL

Pei-Jie Cao, K Kirk Shung

Department of Biomedical Engineerin, University of Southern California, CA, 90089, U.S.A.

Tel: 213-740-9228, Fax: 213-740-0343.

Jei.Cao@bsci.com kkshung@usc.edu

ABSTRACT

A faster and more accurate method for the detection of corneal thickness using an ultrasonic pulse-echo technique was proposed. The corneal thickness was calculated from the time interval between the two echoes reflected at front and rear interfaces of the cornea. The time interval between two echoes was obtained by detecting the peaks of the digitized echoes. A phase-adjusting method, which is superior to the often-used interpolation approach, was used to improve the time resolution to 1/20 of the sampling period. Simulation studies showed this method is comparable to the interpolation method in accuracy at a majority of signal to noise conditions and dynamic ranges of the A/D converter but much easier to implement. The algorithm was implemented in a MCS-8031 microprocessor based pachymeter for measuring corneal thickness. The center frequency of the ultrasonic transducer was 30MHz and the echoes were digitized at a 180MHz sampling frequency. The device showed an accuracy of 1 μm for 10 repeated measurements.

Keywords: ultrasound, corneal thickness, pachymeter, rf signal.

1. INTRODUCTION

It is important to accurately measure the corneal thickness before and after corneal surgeries. For example, in radial keratotomy (RK) to correct myopia (near-sightedness), a series of radial incisions of precise depth is performed on the cornea, resulting in a change in its curvature and hence its refractive power. The depth, length and number of incisions were determined by the degree of optical correction desired. Inadequate depth will result in under-correction, while excessive depth causes over-correction. Therefore an accurate measurement of the corneal thickness is crucial to the success of RK and other surgeries involving the reshaping of the cornea (Wallace, 1989).

Corneal thickness can be measured by optical (Rudoff, 1998) or ultrasonic methods (Wallace, 1989, Hutchison, 1986). The ultrasound method used here is the well-known pulse-echo distance measurement technique (Shung, 1992). The device, known as a "pachymeter," includes a transducer, a signal processing circuit and a display unit. The transducer is specially designed with a polished flat tip so that it can be in direct contact with the cornea surface. In a single A-scan, two echoes are obtained from the front and rear surfaces of the cornea after a very narrow pulse, usually only containing one main cycle, is transmitted perpendicular to the cornea. The time between the two echoes is precisely measured by starting and stopping a high-speed digital counter upon reception of the first and the second echo. The echo can be detected by a threshold method. Once the time difference is known, the thickness of the cornea can be computed by

$$D = Tc / 2, \quad (1)$$

where T is the time interval and c is the sound velocity in the cornea. From equation (1), it is clear that the resolution of the corneal thickness measurement is linearly dependent on that of the time difference measurement. In a system of this design, both the accuracy and resolution of the corneal thickness measurement depend critically on the frequency of the digital counter, and the measured value of T can only be an integer multiple of the counter's period. To measure the thickness with a resolution of 1 μm , the counter has to work at a frequency above 700MHz, which is unrealistic and difficult to design using contemporary circuit design methods and components.

On the other hand, if the echoes are digitized at radio frequency (rf), it is possible to increase the resolution of the thickness measurement without increasing the sampling/counting rate by interpolating the data before processing it. The result is an offline copy of the received signal with a much smaller sampling interval; the positions of the echo peaks can now be determined with higher resolution by examining this interpolated signal. Furthermore, more advanced signal processing techniques such as cross-correlation (Hasegawa, 1999), or wavelet transform techniques can be applied to obtain the time interval (Angrisani, 2000). However, these techniques require large amounts of computation; methods with lighter computational requirements are more desirable for implementation in embedded systems.

In this study, a phase-adjusting method instead of interpolation was introduced to improve the time resolution of the measurements. The results obtained from both methods were compared at different signal to noise ratios (SNR) and the influence of quantification error from A/D converters on their performances was also analyzed. Finally, the implementation of the algorithm in a microprocessor system was described and experimental results were given.

2. METHODS

Referring to Fig. 1, curves S1 and S2 are assumed to be echoes from front and rear surfaces of cornea. The time interval between S1 and S2, can be measured by the time interval between the two peaks P1 and P2. However, due to the finite nonzero sampling period, the maximum points of the digital samples (B1 and B2) may not be truly representative of the original locations of peaks P1 and P2. B1 and B2 represent the points nearest to the true peaks. B1 and B2 are easy to locate by searching for the maximum values of the digital samples. The time interval between them is an integer multiple of the sampling period. If the time interval between B1 and B2 was taken as an estimate of the time difference between the peaks, the estimate would have a worst-case error of one sampling period.

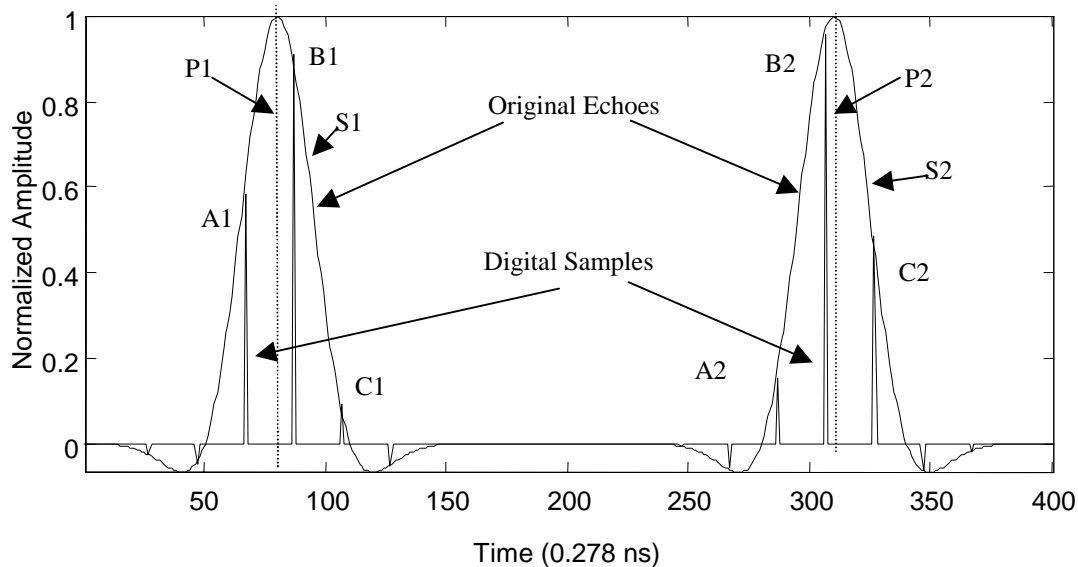


Figure 1. Relation between the digital samples and the real analog echoes

To reduce this error, it is necessary to find a better method to estimate the locations of the true peaks from the sampled signal. This can be achieved by interpolating the digital signal to a higher sampling frequency, and taking the maxima of the interpolated digital signal as the true peak positions. However, as mentioned previously, this method requires heavy computational resources, and is not economical to implement in an embedded real-time system. As an alternative, we can estimate the true positions of the peaks by applying simple trigonometric analysis to the digital samples near the peaks.

To simplify the problem, we only consider the case in which the peak of the digitized signal is on the right side (i.e. after) of the true peak. The pulse transmitted by an acoustic transducer is well approximated

by a Gaussian modulated sinusoid (Abeyratne, 1996). Near the peak, the curve can be modeled as the product of a sinusoid and a Gaussian envelope,

$$R(t) = A \cos(2\pi ft) \exp(-t^2 / \sigma^2). \tag{2}$$

If the time t is assumed to be zero at the true peak position, then:

$$A_1 = A \cos(-2\pi f / f_s + \varphi) \exp[-(\frac{\varphi}{2\pi f} - \frac{1}{f_s})^2 / \sigma^2] \tag{3}$$

$$B_1 = A \cos(\varphi) \exp[-(\frac{\varphi}{2\pi f})^2 / \sigma^2] \tag{4}$$

$$C_1 = A \cos(2\pi \frac{f}{f_s} + \varphi) \exp[-(\frac{\varphi}{2\pi f} + \frac{1}{f_s})^2 / \sigma^2], \tag{5}$$

where f and f_s represent signal center frequency and sampling frequency respectively, A is the amplitude of the wave, φ is the phase difference between the peak of the sampled signal B_1 and the true peak P_1 , and φ is a parameter controlling the shape of a Gaussian function, determined by the bandwidth. Since A varies with the gain of the amplifier, we define:

$$K = \frac{B_1 - C_1}{B_1 - A_1} = \frac{\cos(\varphi) \exp[-\frac{\varphi^2}{(4\pi f \sigma)^2}] - \cos(2\pi \frac{f}{f_s} + \varphi) \exp[-\frac{(\varphi + (2\pi f) / f_s)^2}{(4\pi f \sigma)^2}]}{\cos(\varphi) \exp[-\frac{\varphi^2}{(4\pi f \sigma)^2}] - \cos(-2\pi \frac{f}{f_s} + \varphi) \exp[-\frac{(\varphi - (2\pi f) / f_s)^2}{(4\pi f \sigma)^2}]} \tag{6}$$

Because f and f_s are known, K becomes a function of φ ; a method for the experimental determination of φ is described later in this paper. Equation (6) means that the real peak position can be estimated from the digital samples. The time interval Δt between the sampled peak B_1 and the true peak P_1 must be less than or equal to half of the sampling period:

$$-\frac{T_s}{2} \leq \Delta t \leq \frac{T_s}{2}, \tag{7}$$

where $T_s = 1/f_s$. Because $\varphi = 2\pi f \Delta t$, then:

$$-\frac{f}{f_s} \pi \leq \varphi \leq \frac{f}{f_s} \pi. \tag{8}$$

In our study, $\frac{f}{f_s} = \frac{1}{6}$. In this range, K increases monotonically with φ .

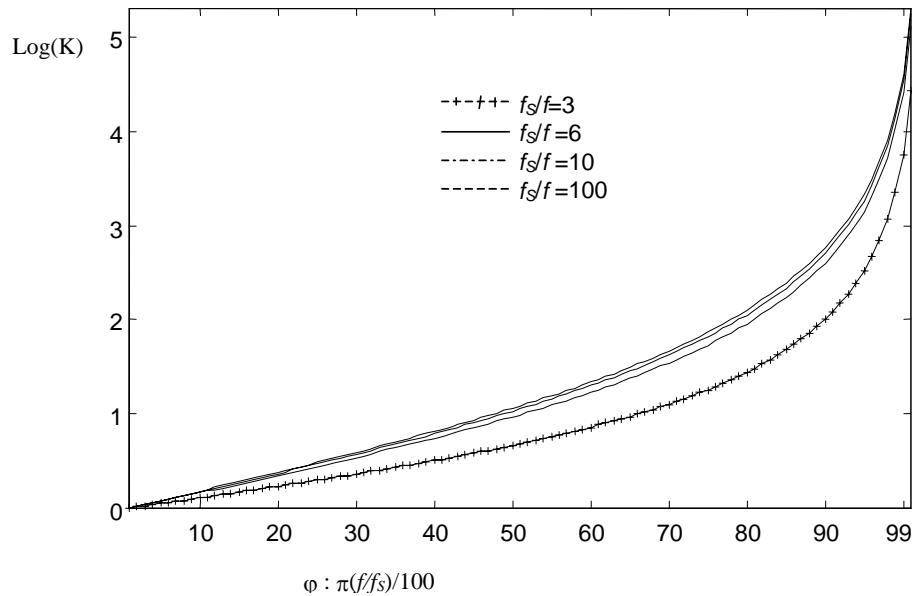


Figure 2. $\log K$ as a function of φ .

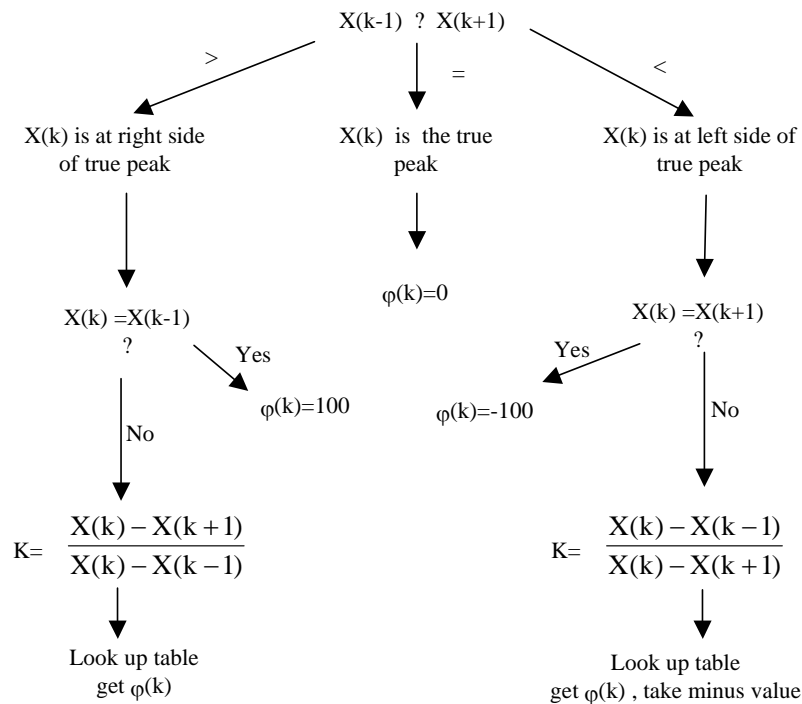


Figure 3. The procedure to determine $\phi(k)$

In Fig. 2, the relation between $\log K$ and ϕ is shown. ϕ increases from zero to $\frac{f}{f_s}\pi$ by 200 steps.

When ϕ equals $\frac{f}{f_s}\pi$, i.e., the true peak is exactly at center between the two digital samples, the amplitudes of A1 and B1 are identical and K will go to infinity. Note that the underlying assumption in the preceding analysis was that the digital peak lies to the right of the true peak; the opposite situation (i.e. where the digital peak falls to the left of the true peak) can be handled in a similar manner, with the exception that ϕ is assigned a negative value.

A step-by-step method for determining the time interval with this method is now presented. It is assumed that $X(n), n=0,1..N$, are the digitized points of the echo and the time interval between two samples is T_s . The relationship between ϕ and K has been stored in a lookup table to save computational resources, and thus make this method fit for use in embedded real-time systems.

Search for the peaks in the digitized signal corresponding to the echoes from the corneal surfaces. Let $X(m)$ and $X(k)$ correspond to the peaks from the front and back surfaces, respectively.

Compute the initial time interval estimation, $T_{int,1} = (k - m)T_s$.

Determine the phase of each peak $\phi(m)$ and $\phi(k)$ in unit of $\pi(f/f_s)/100$ by following the procedure outlined in the flowchart in Figure 3. Compute the final time interval, $T_{int,f} = T_{int,1} - (\phi(m) - \phi(k)) * T_s / (2\pi) / 200$.

3. SIMULATION PROTOCOLS

3.1 Signal generation

A rf signal including two identical echoes was simulated in Matlab 5.3 based on Equ. (2). Both echoes contain a Gaussian envelope with a center frequency of 30MHz. As shown in Fig. 1, the envelope represents the original signal, which was generated at a sampling frequency of 3600MHz. The time unit is the sampling period 0.278ns. The digital samples, representing the output from an A/D converter, were generated at sampling frequency of 180MHz; this frequency will be referred as the A/D sampling frequency. The σ^2 used in Equ. (2) is 6.67.

The true time interval between the peaks of the two echoes in the original signal was 230 time units. Estimating the time interval from the digital samples directly yields a coarse result limited by the time resolution of the ADC. To improve the resolution of the time interval measurement, the digital samples can

either be interpolated to a very high sampling frequency, or processed using the phase-adjusting method described in this paper.

3.2 Using different interpolation methods to improve the time resolution

Using the discrete-time samples shown in Fig.1, the original signal was reconstructed by interpolating to a sampling frequency of 3600 MHz (i.e. a 20x interpolation factor). Several interpolation methods and functions including spline, linear, and cubic methods were compared. The reconstructed signals are shown only near the peaks in Fig. 4; and it is clear that from the peaks of reconstructed signal the spline method is the best whereas the linear is the worst. By interpolation, error can be minimized but cannot be completely eliminated.

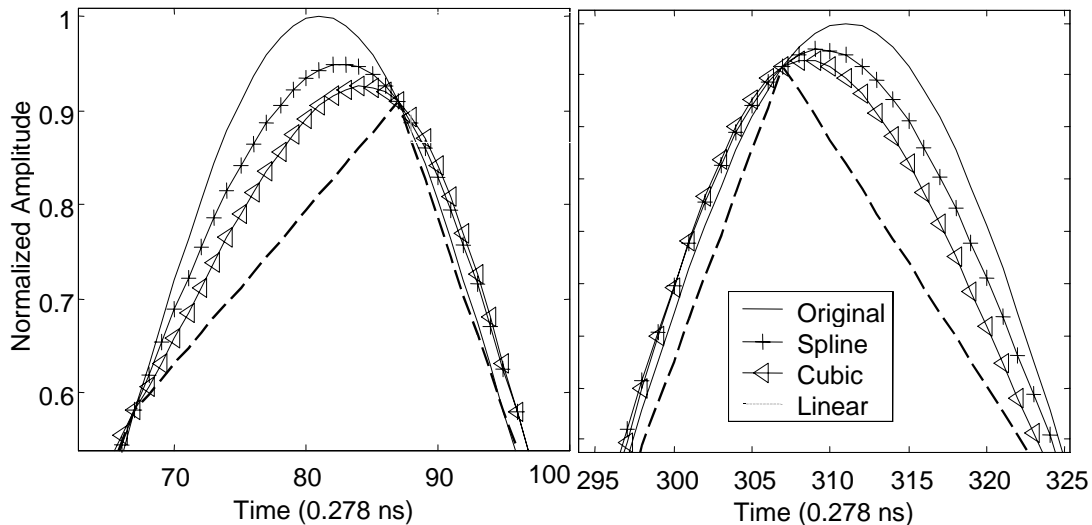


Figure 4. Original signal and reconstructed signal from different interpolation methods.

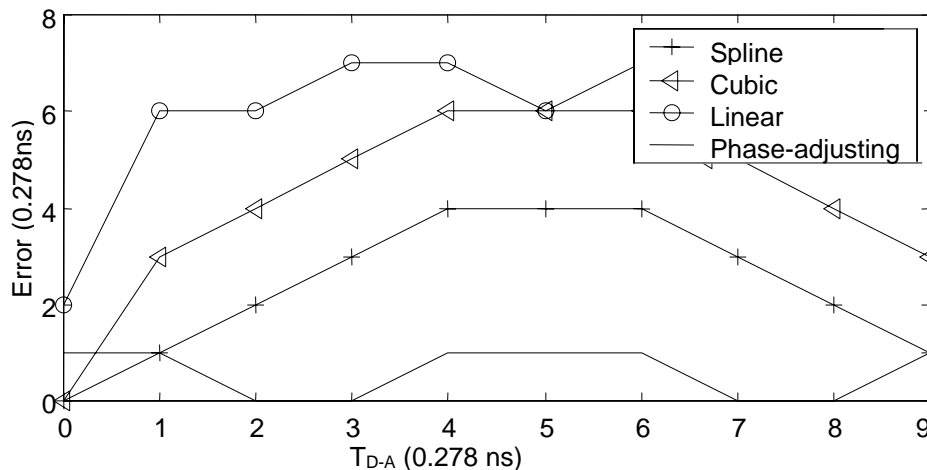


Figure 5. Comparison of time detection errors using different interpolation methods and the phase-adjusting method proposed in this study. Different sets of simulated signal were used. The definition of T_{D-A} is the time delay between the digital peak sampled by an A/D converter and the true original signal peak. It varies between zero and half of the A/D sampling period.

A graphical analysis is given in Fig. 5. The time delay between the digital peak sampled by an A/D converter and the true original signal peak, which is referred to here as T_{D-A} , varies between zero and half of the A/D sampling period. In this simulation series, the original (i.e. continuous-time) signal is represented at 3600MHz, corresponding to 20 times of the A/D sampling frequency. Therefore, the range

of T_{D-A} is from 0 to 9. Ten sets of digital samples were generated with T_{D-A} ranges from 0 to 9. From each set of the digital samples, the original signal was reconstructed by the aforementioned interpolation methods. For the linear interpolation, the results were filtered with a 16th order low pass filter to remove the harmonics. The time interval between the two peaks was detected by peak searching. For the phase-adjusting method, the lookup table of the relation between φ and K based on equation (6) was used. These simulation results reveal that the phase-adjusting method yields smaller time errors than any of the three interpolation methods.

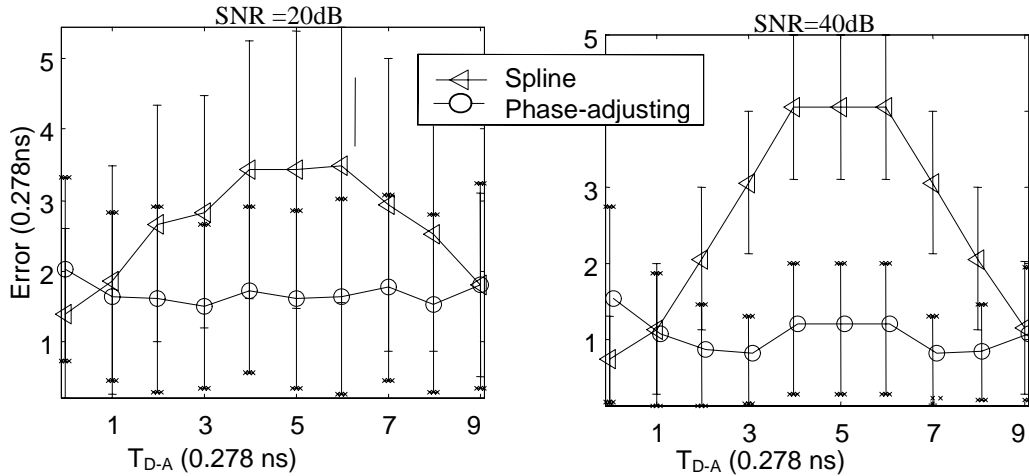


Figure 6. Comparison of results from spline interpolation and phase-adjusting methods at 20dB and 40dB SNR. Different sets of simulated signal were used. The definition of T_{D-A} is the time delay between the digital peak sampled by an A/D converter and the true original signal peak. It varies between zero and half of the A/D sampling period.

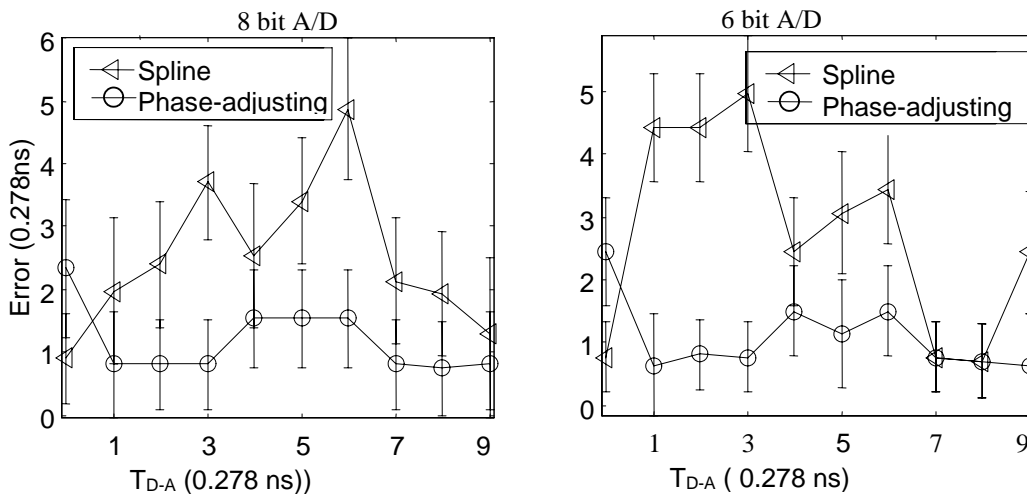


Figure 7. Comparison at different signal dynamic ranges. Different sets of simulated signal were used. The definition of T_{D-A} is the time delay between the digital peak sampled by an A/D converter and the true original signal peak. It varies between zero and half of the A/D sampling period.

3.3 Performance under noisy conditions

The above analysis was conducted under ideal conditions with noiseless signals. Such signals do not exist in the real world; evaluation of the performance of these methods under realistic conditions requires adding noise to the simulated received signal.

Spline interpolation method was chosen to compare with the phase-adjusting method because this method is better than other two interpolation methods. At 20dB and 40dB SNR, experiments were repeated

30 times. At 40dB SNR, the standard deviations from both methods were similar. But at 20dB SNR, the phase-adjusting method yielded a smaller standard deviation.

3.4 Effects of the dynamic range of A/D converter

The limited output resolution of A/D converters must be considered in the design of digital measuring devices. This can be modeled by quantizing the digital signal to 2^n levels, where n is the output resolution of the ADC, in bits. At 40dB SNR, digital samples from 8 bits and 6 bit A/D converters were simulated; the detection results are plotted in Fig. 7. The phase-adjusting method was found to be more robust as well as more accurate than peak detection after the interpolation methods.

4. EXPERIMENTAL RESULTS

4.1 Implementation in a microprocessor system

An ultrasound pachymeter based on above method was developed. The device consists of a transducer with a center frequency of 30MHz and a bandwidth of 15MHz, and an electronic system including amplifiers, a 180MHz A/D converter, an MCS8031 microprocessor and an LCD display screen, as shown in Fig. 8.

The transducer with an aperture of 2mm in diameter is specifically designed with a small f-number of 1 so that the focal depth (2mm) is near its surface. The piezo material used is lead titanate. The surface is polished and is intended to be placed in direct contact with the cornea. The transmit voltage is 60 volts. The amplifier has a variable gain from 40dB to 80dB. The A/D converter is 8 bit, working at 180MHz. A first-in-first-out (FIFO) memory was used to store the digitized data for a single pulse echo transmission. The 8031-microprocessor system has 64k bytes Ram and Rom. The echo was shown on the graphic LCD as A-scan line and refreshed at a frequency of 5Hz. When the echoes from both front and rear surfaces of the cornea obtain maximum amplitudes on the LCD display, indicating that the ultrasonic beam was perpendicular to the surface of the cornea, a number of pulse-echoes were collected, digitized and stored in the RAM by pressing a button. The number of repeated measurements was configurable from 5 to 20. The averaged data and standard deviation from the total measurements were shown on the LCD.

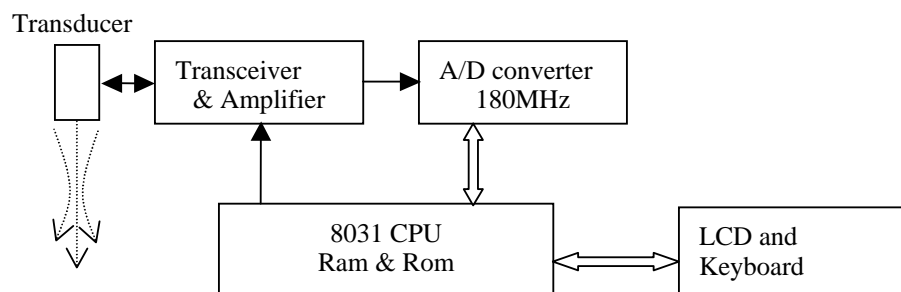


Figure 8. System diagram for the pachymeter

4.2 Lookup table

A lookup table to speed the implementation of the phase-adjusting method can be constructed once certain system parameters are known. These parameters include the Gaussian characteristic σ^2 and the ratio of the center frequency and sampling frequency, f/fs . The σ^2 parameter is related to the bandwidth of the ultrasonic system's signal chain; here, since the electronic components have a much higher bandwidth than the acoustic components, σ^2 is determined by the bandwidth of the transducer alone.

The best way to determine σ^2 is using the Least Mean Square (LMS) method to compare a simulated echo with a digitized one from the practical system. The optimal shape parameter of Gaussian signal is obtained when it gives the LMS error. A real echo from the front surface of a cornea was recorded using a digital oscilloscope and is shown in Fig. 9.

The simulated echoes with $\sigma^2=10, 27$ and 500 were compared with the recorded echo in Fig. 10(a). It was found that the simulated echo with a σ^2 value of 27 matches the recorded one very well within the main lobe range. The computed mean square errors from the simulated echoes with σ^2 varying from 15 to

100 were shown in Fig. 10(b). The LMS error occurred at $\sigma^2=27$ location. In this study, $\sigma^2=27$ was used in construction of the lookup table.

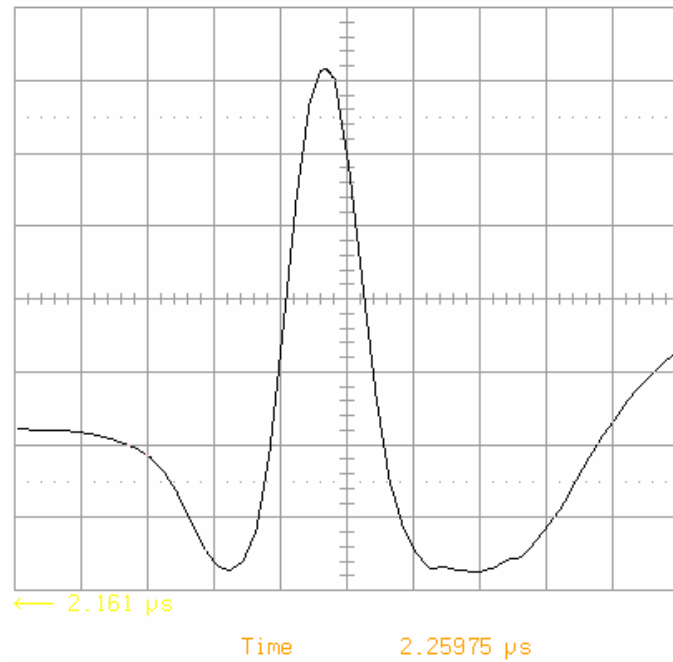


Figure 9. A recorded echo from the front surface of a cornea using a digital oscilloscope.

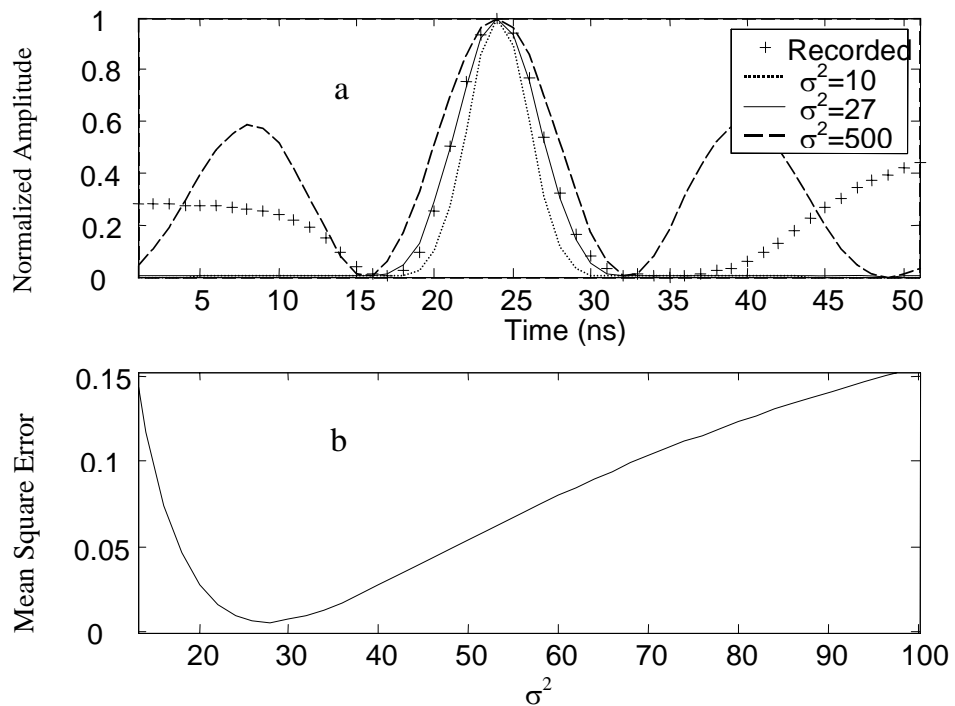


Figure 10. a. Comparison of the simulated echoes with different σ^2 and the recorded one by digital oscilloscope. b. The computed mean square error from the simulated echoes with σ^2 varies from 15 to 100.

4.3 Experimental setup

A flat Plexiglas sample with $563.6 \pm 1.3 \mu\text{m}$ thickness was used as a phantom for these experiments. The sound velocity in Plexiglas is 2730m/s. Two groups of experiments were performed. In the first group,

the transducer was in direct contact with the surface of the sample, while in the second group, the transducer was positioned about 0.5 mm from the surface of the sample. Acoustic coupling gel was used in both groups of experiments to eliminate air gaps which would otherwise lead to spurious echoes. Because a negative pulse was transmitted to the transducer, the echo from the rear surface of the sample will be positive and the echo from the front surface depends on the measure methods. If the transducer is in direct contact with the surface, the echo will be positive because of the higher impedance of the matching layer of the transducer, otherwise, it will be negative. So when the non-contact method was used, the echo from the front surface was reversed by software.

In each group of experiments, three data sets were acquired. In each set, ten measurements were taken; each measurement was computed as the average of ten pulse-echo scan results. The transducer was removed and repositioned between data sets; the purpose of this was to test the precision (i.e. repeatability) of the measurement process. The results of these experiments are shown in Table 1.

It is apparent from the above results that there is very little variation in measurement results in the second group of experiments, revealing that the measurement process is repeatable when the transducer is not in contact with the specimen. The case in which the transducer directly contacts the specimen reveals a small yet statistically significant variation in measurement results among different tests.

Table 1. Measured thickness and standard deviation from different groups.

Group		Subgroup 1	Subgroup 2	Subgroup 3
Contact	Mean(μm)	563	567	568
	Std(μm)	1	1	2
Non-contact	Mean(μm)	564	563	564
	Std(μm)	2	1	2

5. DISCUSSION

5.1 Limitations of the algorithm

The essential problem in this study is peak position estimation from its digital samples. Theoretically, the real signal can be reconstructed from its digital samples when the sampling frequency is higher than twice that of the highest frequency component of the signal. However, the algorithms for these processing techniques are generally memory-intensive and compute-intensive operations that cannot be implemented in modest microcontroller hardware. Therefore, barring major optimizations in the algorithms for their implementation, these techniques are not appropriate for embedded implementation.

The phase-adjusting method is by no means perfect, but it has the advantage of resulting less computing and having similar or even better worst-case accuracy under the same conditions compared to the interpolation methods. Because interpolation methods have intrinsic defects, they are not sensitive to certain noise conditions, such as 20dB SNR, which is frequently encountered in ultrasound systems. Fig. 6 shows that the performance of the interpolation methods is similar at 20dB and 40dB SNR. The phase-adjusting method is more sensitive to noise; its performance is significantly worse at 20dB SNR than that at 40dB SNR. However, it is fortunate that in cornea thickness measurement, low SNR is not a matter of concern because the reflected echoes usually have very high amplitudes.

It is also clear from Figures 5 and 7 that the A/D converter resolution affects all methods tested in this study. However, the results show that 8-bit and 6-bit A/D conversion both yield similar results from the phase-adjusting algorithm.

5.2 Influence of center frequency and the sampling frequency

In this study, a 30MHz center frequency and 180MHz sampling frequency were used. It is necessary to analyze the effects of these two frequencies. If a lower center frequency such as 15MHz was used, and the sampling frequency remained the same, the difference between the digital peak and its adjacent samples become smaller, as shown in Fig. 11. It is shown in Fig 3, that the value of K is sensitive to noise. The performance of the algorithm will decrease at the same A/D dynamic range and SNR. If the sampling frequency is decreased to 60MHz, the time period between two adjacent digital samples became twice long. A lookup table of φ -K relation which doubles the fine steps is needed to achieve the same time resolution.

However, the calculated K always has a fluctuation around its real values because of the noise. This fluctuation is determined primarily by SNR. A smaller K step in the lookup table means more sensitive to the noise. For a fixed SNR, the higher center frequency and sampling frequency the better the algorithm performance.

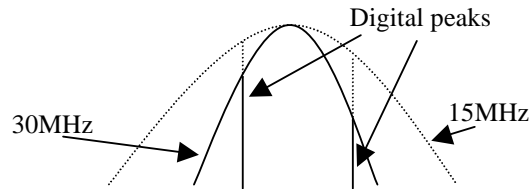


Figure 11. The difference between the digital peak and its adjacent samples becomes smaller when center frequency decreases from 30MHz to 15MHz.

5.3 Threshold detection and peak detection

In a practical pulse-echo system, the amplitude of the echo is affected by the transmitted pulse, the acoustic impedance difference at the interface, and the electronics of system. In this case, the location of the echo is better represented by its peak position than the position at which the echo meets a certain threshold level. In a pure analog system, it is easier to detect the edge of the echo by threshold but more difficult to detect the peak location directly. Using a differential circuit, the peak point can be converted to a zero-crossing point, and peak detection becomes a zero-crossing detection. Because of the echo has more than one zero-crossing points; it is not easy to remove the false ones.

5.4 Contact measurement and non-contact measurement

The results in Table 1 show that the measurement results are strongly repeatable provided that the transducer is not moved between measurements. The precision of the results decreases when the transducer is moved and repositioned between measurements; this repetition error is reduced when the transducer is not in direct contact with the cornea.

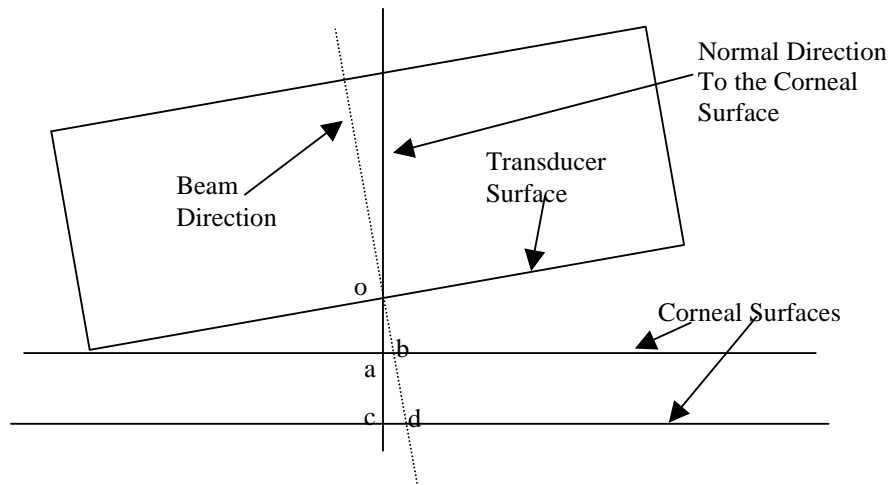


Figure 12. Error from malposition in contact and non-contact methods

Figure 12 shows the origin of this error. To obtain a correct thickness measurement, good contact between the transducer surface and the corneal front surface must be maintained when the contact measurement method is used; gaps must not be allowed to form between the specimen and the transducer. In these experiments, since both surfaces were rigid, a small error in the angle between the two surfaces may occur resulting in a gap at center of the transducer surface with a length of OB as shown in Fig. 12. In the case of a 0.5° misalignment, the gap measures $ob=1.5\sin(0.5^\circ)=0.0131\text{mm}$. The wavelength of

ultrasound pulse at 30MHz is longer than 30 μ m, and this small gap causes a compound echo. Thus an error of 13 μ m was induced.

In the case of a non-contact measurement setup, there is a distance between the transducer and the cornea; this distance helps suppress spurious effects of alignment errors. From Figure 12, the error is simply the difference between the lengths of BD and AC; this difference is significantly smaller for a given angle than OB. For example, this difference is about 2.3 μ m for a 5 degree angle misalignment; this is significantly better than the result from the contact method. We hence concluded that the non-contact method should be used, provided that the signal-to-noise ratio of the transducer and system is sufficiently high.

6. CONCLUSION

Being able to measure the time interval between two echoes from the front and rear surface of cornea at high resolution is critical to the accurate measurement of corneal thickness using ultrasound pulse-echo method. The current study shows that at normal SNR condition, the phase-adjusting method proposed has a similar or better performance than interpolation based methods but much lower computational complexity to estimate the location of the true echo peaks from their digital samples. The algorithm was implemented in a microprocessor-based pachymeter, and accurate, highly repeatable results were achieved using this signal processing method.

ACKNOWLEDGMENTS

This work has been supported by NIH grant # P41-RR11795

REFERENCES

- Wallace D.A., Hills B., Feldon S.E., Digital ultrasonic instrument for ophthalmic use. Unite States Patents, Patent Number 4,817,432. Apr. 4, 1989.
- Rudoff W., Matthias B., Ronald G. (1998) Rapid and precise in vivo measurement of human corneal thickness with optical low-coherence reflectometry in normal human eyes. *Journal of Biomedical Optics*, **3**: 253-258.
- Hutchison S., Kirkwood, Ritter J.A. Ultrasonic System for Obtaining Ocular measurements," Unite States patent, Patent Number 4,564,018, Stephen Hutchison, et al. Jan. 14, 1986.
- Shung K.K., Smith M.B., Tsui B.M.W. (1992) Principles of medical imaging. San Diego : Academic Press.
- Hasegawa H., Kanai H., Hosimiya N., Koiwa Y. (1999) Reduction of influence of decrease in SNR of ultrasonic pulse during cardiac cycle in measurement of small change in thickness of arterial wall. *IEEE ultrasonic symposium*, pp.1-4.
- Angrisani L., Daponte P., D'Apuzzo M. (2000) The detection of echoes from multilayer structures using the wavelet transform. *IEEE Trans on Instrumentation and Measurement*, **49**:727-731.
- Abeyratne U.R., Petropulu A.P., Reid J.M. (1996) On modeling the tissue response from ultrasonic B-scan images. *IEEE Transactions on Medical Imaging*, **15**:479-490.

Received: August 25th 2003

Accepted in final format: September 25th 2004 after one revision

About the authors

Pei-Jie Cao was born in China in 1968. He got his master and Ph.D in Biomedical Engineering from Xi'an Jiaotong University in 1999. He worked as a postdoc researcher at NIH Transducer Center, Penn State University. In July 2002, he joined the Biomedical Engineering Department at University of Southern California as research assistant professor with the relocation of the NIH Transducer Center. In Nov. 2003, he moved to Silicon Valley working at Boston Scientific as a senior R&D engineer. His research interests include design and computation of high frequency ultrasound transducer, ultrasound system development, and intravascular ultrasound. He can be reached at Jei.Cao@bsci.com.

K. Kirk Shung is a professor of Biomedical Engineering at University of Southern California. His research interests are in ultrasonic imaging and tissue characterization, ultrasonic contrast agents and their applications in ultrasonic imaging and blood flow measurements, ultrasonic transducers and arrays. He can be reached at kkshung@usc.edu.